

The magnetostriction of Tb, Dy and Ho revisited

This article has been downloaded from IOPscience. Please scroll down to see the full text article.

2004 J. Phys.: Condens. Matter 16 7151

(<http://iopscience.iop.org/0953-8984/16/39/046>)

View [the table of contents for this issue](#), or go to the [journal homepage](#) for more

Download details:

IP Address: 129.252.86.83

The article was downloaded on 27/05/2010 at 18:01

Please note that [terms and conditions apply](#).

The magnetostriction of Tb, Dy and Ho revisited

L Benito, J I Arnaudas¹, M Ciria, C de la Fuente and A del Moral

Departamento de Magnetismo de Sólidos, Departamento de Física de la Materia Condensada—ICMA, Universidad de Zaragoza—CSIC, 50071 Zaragoza, Spain

Received 8 April 2004

Published 17 September 2004

Online at stacks.iop.org/JPhysCM/16/7151

doi:10.1088/0953-8984/16/39/046

Abstract

In this paper we present re-analyses of magnetostriction measurements earlier performed in terbium, dysprosium and holmium single crystals. In the framework of the standard theory of single-ion crystal-electric-field and two-ion exchange magnetostrictions, we explain the thermal variation of the anisotropic saturation magnetostriction within the basal plane by considering high-order terms in the magnetoelastic energy. Using complementary basal-plane magnetic anisotropy measurements, we have been able to obtain the second- and fourth-order magnetoelastic coupling parameters associated with the orthorhombic distortion of the hexagonal plane for the above-mentioned three heavy rare earths.

1. Introduction and outlook of theory

The magnetoelastic behaviour of metallic rare earths (RE) was thoroughly studied in the 1960s [1–3], mainly motivated by the large values of magnetostrictive strains measured in some of them. The effects of such a large magnetoelastic coupling on the magnetic structure and properties of these elements also attracted great interest (see [4] and references therein), which has been more recently renovated with the appearance of artificially grown high-quality RE-based films and superlattices (see e.g. [5] and references therein). In these systems, alterations in the magnetoelastic behaviour due to the presence of interfaces and growing stresses have also been found [6, 7].

In general, the analysis of the effects associated with the deformations of the crystal lattice, via the spin–orbit coupling, is made by using the so-called *standard theory of magnetostriction* [8, 9], which is usually enough to explain the experimental facts. This was the approach taken by the authors who made the magnetostriction measurements in Tb and Dy to interpret their results (see [10] and references therein). Concerning the temperature dependence of the magnetostriction coefficients, the single-ion mean-field model gave reasonable agreement at not too low temperatures, mainly for the basal plane distortions in Tb and Dy. For these elements, the magnetostriction at the paramagnetic regime was analysed and the strain

¹ Author to whom correspondence should be addressed.

dependence of the exchange interaction was evidenced [11], which indicates the necessity of including the exchange magnetostriction in the interpretation of experimental data. For Ho, the magnetoelastic behaviour is more complex and no theoretical analyses of the magnetostriction experiments, by means of the standard model, can be found in the literature. However, even for Tb and Dy, it is worth stressing that the explanation of the experimental results using the standard theory of magnetostriction was not fully satisfactory.

We should mention that, in previous years, significant effort has been made to explain the magnetostriction of RE and RE intermetallics by using numerical methods. Magnetization isotherms in Ho have been calculated [12] via a self-consistent mean-field method [4] which, including the exchange magnetostriction, has been employed to explain the *c*-axis distortion as a function of the magnetic field and temperature, as well as the lattice modulation observed in x-ray diffraction experiments [12]. Other kinds of advanced numerical analyses have been performed in RECu₂ intermetallics, where mean-field Monte Carlo simulations [13, 14] showed that the exchange and single-ion contributions to the magnetostriction were of the same order of magnitude. This is not the case for other RE elements; for instance, *ab-initio* calculations in Tb and Er [15] showed that the giant magnetostriction of these elements is dominated by the single-ion 4f crystal electric field (CEF) contribution. As we shall see below, our results confirm this fact in Tb as well as in Dy; however, in Ho, the exchange magnetostriction has a significant contribution.

Finally, we would like to point out that, although a large amount of work has already been done to understand the magnetoelastic properties of RE elements, the extension to the whole RE series and experiments under larger applied magnetic fields are yet to be carried out.

We will review in the rest of this section the basics of the theory through which we have performed our analysis of the magnetostrictive distortions. To obtain the expressions of the equilibrium strains, which we will compare later with the experimentally determined ones, we should minimize the sum of elastic plus magnetoelastic free-energy densities. The first term is written classically and the magnetoelastic free energy is obtained by performing the thermal average of the magnetoelastic Hamiltonian over the ground-level states of the system (see e.g. [4, 9]). The temperature dependencies coming from the different terms that contribute to a given strain, can be easily discerned if we group the elastic and magnetoelastic energy terms associated with the different irreducible strains compatible with the hexagonal symmetry and, then, perform all the calculations (note that the hexagonal symmetry of the system is assumed to be only slightly distorted by the magnetostrictive deformations). According to this, and summing up over the ions, N , we write, in a coordinate system (ξ, η, ζ) parallel to the *a*-, *b*- and *c*-directions of the hcp crystal lattice, the following magnetoelastic Hamiltonian terms:

$$\begin{aligned}
 \mathcal{H}^\alpha &= \mathcal{H}_{me}^\alpha + \mathcal{H}_{el}^\alpha \\
 &= - \sum_{i=1}^N \left[\sum_{l=2,4,6} \{ \tilde{B}'_{\alpha 1} \varepsilon_{\alpha 1} + \tilde{B}'_{\alpha 2} \varepsilon_{\alpha 2} \} Q_l^0(\mathbf{J}_i) + \{ \tilde{B}^{66}_{\alpha 1} \varepsilon_{\alpha 1} + \tilde{B}^{66}_{\alpha 2} \varepsilon_{\alpha 2} \} Q_6^0(\mathbf{J}_i) \right. \\
 &\quad \left. + \sum_{j>i} \{ \tilde{D}'_{\alpha 1}(ij) \varepsilon_{\alpha 1} + \tilde{D}'_{\alpha 2}(ij) \varepsilon_{\alpha 2} \} \mathbf{J}_i \cdot \mathbf{J}_j + \{ \tilde{D}'_{\alpha 1}(ij) \varepsilon_{\alpha 1} + \tilde{D}'_{\alpha 2}(ij) \varepsilon_{\alpha 2} \} J_{i\xi} J_{j\xi} \right] \\
 &\quad + N \left(\frac{1}{2} c_{\alpha 1} \varepsilon_{\alpha 1}^2 - c_{\alpha 3} \varepsilon_{\alpha 1} \varepsilon_{\alpha 2} + \frac{1}{2} c_{\alpha 2} \varepsilon_{\alpha 2}^2 \right), \tag{1}
 \end{aligned}$$

related to the α -strains $\varepsilon_{\alpha 1} = \varepsilon_{\xi\xi} + \varepsilon_{\eta\eta} + \varepsilon_{\zeta\zeta}$ (isotropic volume deformation) and $\varepsilon_{\alpha 2} = \frac{1}{3}(2\varepsilon_{\xi\xi} - \varepsilon_{\eta\eta} - \varepsilon_{\zeta\zeta})$ (change of the \mathbf{c}/\mathbf{a} axes ratio), $\varepsilon_{\xi\xi}$, $\varepsilon_{\eta\eta}$ and $\varepsilon_{\zeta\zeta}$ being the Cartesian strains,

$$\begin{aligned} \mathcal{H}^\gamma &= \mathcal{H}_{me}^\gamma + \mathcal{H}_{el}^\gamma \\ &= - \sum_{i=1}^N \left[\sum_{l=2,4,6} \tilde{B}_{\gamma 2}^l \{ \varepsilon_{\gamma 1} Q_l^2(\mathbf{J}_i) + \varepsilon_{\gamma 2} Q_l^{-2}(\mathbf{J}_i) \} + \sum_{l=4,6} \tilde{B}_{\gamma 4}^l \{ \varepsilon_{\gamma 1} Q_l^4(\mathbf{J}_i) + \varepsilon_{\gamma 2} Q_l^{-4}(\mathbf{J}_i) \} \right. \\ &\quad \left. + \frac{1}{2} \sum_{j>i} \{ \tilde{D}_{\gamma 1}(ij) \varepsilon_{\gamma 1} (J_{i\xi} J_{j\xi} - J_{i\eta} J_{j\eta}) + \tilde{D}_{\gamma 2}(ij) \varepsilon_{\gamma 2} (J_{i\xi} J_{j\eta} + J_{i\eta} J_{j\xi}) \} \right] \\ &\quad + \frac{1}{2} c_\gamma N (\varepsilon_{\gamma 1}^2 + \varepsilon_{\gamma 2}^2), \end{aligned} \quad (2)$$

related to the basal-plane hexagonal symmetry-breaking γ -strains $\varepsilon_{\gamma 1} = \frac{1}{2}(\varepsilon_{\xi\xi} - \varepsilon_{\eta\eta})$, i.e. (orthorhombic strain) and $\varepsilon_{\gamma 2} = \varepsilon_{\xi\eta}$ (basal plane shear strain) and

$$\begin{aligned} \mathcal{H}^\varepsilon &= \mathcal{H}_{me}^\varepsilon + \mathcal{H}_{el}^\varepsilon = - \sum_{i=1}^{i=N} \left[\sum_{l=2,4,6} \tilde{B}_{\varepsilon 1}^l \{ Q_l^1(\mathbf{J}_i) \varepsilon_{\varepsilon 1} + Q_l^{-1}(\mathbf{J}_i) \varepsilon_{\varepsilon 2} \} \right. \\ &\quad \left. + \tilde{B}_{\varepsilon 5} \{ Q_6^5(\mathbf{J}_i) \varepsilon_{\varepsilon 1} - Q_6^{-5}(\mathbf{J}_i) \varepsilon_{\varepsilon 2} \} \right. \\ &\quad \left. + \frac{1}{2} \sum_{j>i} \{ \tilde{D}_{\varepsilon 1}(ij) \varepsilon_{\varepsilon 1} (J_{i\zeta} J_{j\xi} + J_{i\xi} J_{j\zeta}) + \tilde{D}_{\varepsilon 2}(ij) \varepsilon_{\varepsilon 2} (J_{i\eta} J_{j\zeta} + J_{i\zeta} J_{j\eta}) \} \right] \\ &\quad + \frac{1}{2} c_\varepsilon N (\varepsilon_{\varepsilon 1}^2 + \varepsilon_{\varepsilon 2}^2), \end{aligned} \quad (3)$$

associated with the \mathbf{c} -axis shear strains $\varepsilon_{\varepsilon 1} = \varepsilon_{\xi\zeta}$ and $\varepsilon_{\varepsilon 2} = \varepsilon_{\eta\zeta}$. In the above expressions, \tilde{B}_Γ^l , $\tilde{D}_\Gamma(ij)$ and c_Γ are, respectively, crystal-field magnetoelastic coupling parameters, exchange magnetoelastic coupling parameters and irreducible elastic constants, all per ion, with Q_l^m being Stevens operators and (J_ξ, J_η, J_ζ) the angular momentum operators. Notice that the two-ion exchange contributions have been considered only up to second order.

Now, minimization with respect to the irreducible strains and thermal average of the spin operators, i.e. $\langle \partial \mathcal{H}^\Gamma / \partial \varepsilon_\Gamma \rangle_T = 0$, would give us the equilibrium values of the strains, $\bar{\varepsilon}_\Gamma$. However, the Hamiltonians used were written considering that $\zeta \parallel \mathbf{c}$ is the quantization axis but, on applying a magnetic field parallel to some arbitrary direction $\hat{\mathbf{u}}$, the saturation magnetization can become aligned parallel to $\hat{\mathbf{u}}$. If we choose a new (x, y, z) coordinate system, such as $\hat{\mathbf{z}} \parallel \hat{\mathbf{u}}$, forming angles (θ, ϕ) in the (ξ, η, ζ) system and $\hat{\eta}$ being within the basal plane of the hcp structure, the Stevens operators $Q_l^m(\mathbf{J}_i)$ can be written in the new system as: $Q_l^m(\mathbf{J}_i) = \sum_{m'} \langle Y_l^{m'} | Q_l^m \rangle Y_l^{m'}(\mathbf{J}_i)$ [8, 16], where $Y_l^{m'}(\mathbf{J}_i)$ are spherical tensor operators. Since $Y_l^m(\mathbf{J}_i)$ possesses cylindrical symmetry around $\hat{\mathbf{u}}$, their thermal averages essentially cancel, except when $m = 0$ [8]. Thus, $\langle Q_l^m(\mathbf{J}_i) \rangle_T \propto b_l^m \langle O_l^0(\mathbf{J}_i) \rangle_T$, where the $b_l^m \propto P_l^m(\cos \theta) \cos(m\phi)$, for $m > 0$ and $b_l^m \propto P_l^{|m|}(\cos \theta) \sin(|m|\phi)$, for $m < 0$, $P_l^m(\cos \theta)$ being the associated Legendre functions of the first kind [16].

In the new coordinate system, the equilibrium irreducible α and γ strains are

$$\begin{aligned} \bar{\varepsilon}_{\alpha 1} &= \lambda_{1,2}^\alpha + \lambda_{1,4}^\alpha + \lambda_{1,6}^\alpha + \lambda_{1,66}^\alpha \cos 6\phi + \eta_{1,1}^\alpha \sin 2\phi + \eta_{1,2}^\alpha \cos 2\phi + \eta_{1,0}^\alpha, \\ \bar{\varepsilon}_{\alpha 2} &= \lambda_{2,2}^\alpha + \lambda_{2,4}^\alpha + \lambda_{2,6}^\alpha + \lambda_{2,66}^\alpha \cos 6\phi + \eta_{2,1}^\alpha \sin 2\phi + \eta_{2,2}^\alpha \cos 2\phi + \eta_{2,0}^\alpha, \\ \bar{\varepsilon}_{\gamma 1} &= (\lambda^{\gamma 2} + \eta_1^{\gamma 1}) \cos 2\phi + \eta_0^\gamma \sin 2\phi + \lambda^{\gamma 4} \cos 4\phi + \eta_0^\gamma \\ \bar{\varepsilon}_{\gamma 2} &= (\lambda^{\gamma 2} + \eta_1^{\gamma 2}) \sin 2\phi + \eta_2^\gamma \cos 2\phi - \lambda^{\gamma 4} \sin 4\phi + \eta_2^\gamma, \end{aligned} \quad (4)$$

where magnetostriction coefficients λ and η are defined in terms of magnetoelastic coupling parameters and irreducible elastic constants:

$$\begin{aligned}
 \lambda_{1,l}^\alpha &= \frac{1}{c_{\alpha 1} c_{\alpha 2} - c_{\alpha 3}^2} (\tilde{B}_{\alpha 1}^l c_{\alpha 2} - \tilde{B}_{\alpha 2}^l c_{\alpha 3}) P_l^0(\cos \theta) \langle O_l^0 \rangle_T, \quad l = 2, 4, 6, \\
 \lambda_{1,66}^\alpha &= \frac{1}{c_{\alpha 1} c_{\alpha 2} - c_{\alpha 3}^2} (\tilde{B}_{\alpha 1}^{66} c_{\alpha 2} - \tilde{B}_{\alpha 2}^{66} c_{\alpha 3}) \sin^6 \theta \langle O_6^0 \rangle_T, \\
 \lambda_{2,l}^\alpha &= \frac{1}{c_{\alpha 1} c_{\alpha 2} - c_{\alpha 3}^2} (\tilde{B}_{\alpha 2}^l c_{\alpha 1} - \tilde{B}_{\alpha 1}^l c_{\alpha 3}) P_l^0(\cos \theta) \langle O_l^0 \rangle_T, \quad l = 2, 4, 6, \\
 \lambda_{2,66}^\alpha &= \frac{1}{c_{\alpha 1} c_{\alpha 2} - c_{\alpha 3}^2} (\tilde{B}_{\alpha 2}^{66} c_{\alpha 1} - \tilde{B}_{\alpha 1}^{66} c_{\alpha 3}) \sin^6 \theta \langle O_6^0 \rangle_T, \\
 \eta_{2,1}^{\alpha} &= \frac{1}{2(c_{\alpha 1} c_{\alpha 2} - c_{\alpha 3}^2)} \sum_{j>i} \left[\left(\tilde{D}_{\alpha 1}(ij) c_{\alpha 2} - \tilde{D}_{\alpha 2}(ij) c_{\alpha 3} \right) (\langle J_{yi} J_{zj} + J_{zi} J_{yj} \rangle_T P_1^1(\cos \theta) \right. \\
 &\quad \left. - \langle J_{xi} J_{yj} + J_{yi} J_{xj} \rangle_T P_1^0(\cos \theta) \right), \\
 \eta_{2,2}^{\alpha} &= \frac{1}{2(c_{\alpha 1} c_{\alpha 2} - c_{\alpha 3}^2)} \sum_{j>i} \left[\left(\tilde{D}_{\alpha 1}(ij) c_{\alpha 2} - \tilde{D}_{\alpha 2}(ij) c_{\alpha 3} \right) (\langle J_{yi} J_{zj} + J_{zi} J_{yj} \rangle_T P_1^1(\cos \theta) \right. \\
 &\quad \left. - \langle J_{xi} J_{yj} + J_{yi} J_{xj} \rangle_T P_1^0(\cos \theta) - 2 \langle J_{yi} J_{yj} \rangle_T \right), \\
 \eta_{2,0}^{\alpha} &= \frac{1}{c_{\alpha 1} c_{\alpha 2} - c_{\alpha 3}^2} \sum_{j>i} \left\{ \left(\tilde{D}'_{\alpha 1}(ij) c_{\alpha 2} - \tilde{D}'_{\alpha 2}(ij) c_{\alpha 3} \right) (\langle J_{xi} J_{xj} - J_{zi} J_{zj} \rangle_T P_2^2(\cos \theta) / 3 \right. \\
 &\quad \left. + \langle J_{zi} J_{xj} + J_{xi} J_{zj} \rangle_T P_2^1(\cos \theta) / 3) - (1/2) (\tilde{D}_{\alpha 1}(ij) c_{\alpha 2} - \tilde{D}_{\alpha 2}(ij) c_{\alpha 3}) \right. \\
 &\quad \left. \times (\langle J_{zi} J_{yj} + J_{yi} J_{zj} \rangle_T P_1^1(\cos \theta) + \langle J_{xi} J_{yj} + J_{yi} J_{xj} \rangle_T P_1^0(\cos \theta) + \langle \mathbf{J}_i \cdot \mathbf{J}_j \rangle_T) \right\}, \\
 \lambda^{\gamma, 2} &= \frac{1}{c_\gamma} (\tilde{B}_{\gamma 2}^2 P_2^2(\cos \theta) \langle O_2^0 \rangle_T + \tilde{B}_{\gamma 2}^4 P_4^2(\cos \theta) \langle O_4^0 \rangle_T + \tilde{B}_{\gamma 2}^6 P_6^2(\cos \theta) \langle O_6^0 \rangle_T), \\
 \lambda^{\gamma, 4} &= \frac{1}{c_\gamma} (\tilde{B}_{\gamma 4}^4 P_4^4(\cos \theta) \langle O_4^0 \rangle_T + \tilde{B}_{\gamma 4}^6 P_6^4(\cos \theta) \langle O_6^0 \rangle_T), \\
 \eta_1^{\gamma 1} &= \left(\frac{1}{4c^\gamma} \right) \sum_{j>i} \left[\tilde{D}_{\gamma 1}^1(ij) \left\{ 2 \langle J_{zi} J_{zj} \rangle_T P_2^2(\cos \theta) / 3 - 2 \langle J_{zi} J_{xj} + J_{xi} J_{zj} \rangle_T P_2^1(\cos \theta) / 3 \right. \right. \\
 &\quad \left. \left. - \langle J_{zi} J_{yj} + J_{yi} J_{zj} \rangle_T P_1^1(\cos \theta) + 2 \langle J_{xi} J_{xj} \rangle_T P_2^0(\cos \theta) \right. \right. \\
 &\quad \left. \left. + \langle J_{xi} J_{yj} + J_{yi} J_{xj} \rangle_T P_1^0(\cos \theta) \right\} \right], \\
 \eta_0^\gamma &= \left(\frac{1}{4c^\gamma} \right) \sum_{j>i} \tilde{D}_{\gamma 1}(ij) \{ \langle J_{yi} J_{zj} + J_{zi} J_{yj} \rangle_T P_1^1(\cos \theta) - \langle J_{yi} J_{xj} + J_{xi} J_{yj} \rangle_T P_1^0(\cos \theta) \}, \\
 \eta_2^\gamma &= \left(\frac{1}{4c^\gamma} \right) \sum_{j>i} \tilde{D}_{\gamma 2}(ij) \{ \langle J_{yi} J_{zj} + J_{zi} J_{yj} \rangle_T P_1^1(\cos \theta) - \langle J_{yi} J_{xj} + J_{xi} J_{yj} \rangle_T P_1^0(\cos \theta) \\
 &\quad - 2 \langle J_{yi} J_{yj} \rangle_T \}.
 \end{aligned} \tag{5}$$

By using expressions (4) we can write the Cartesian strains in terms of the magnetostriction coefficients:

$$\begin{aligned}
\bar{\varepsilon}_{\xi\xi} &= \left\{ \left(\frac{1}{3}\eta_{1,1}^\alpha \pm \eta_0^\gamma - \frac{1}{2}\eta_{2,1}^\alpha \right) \sin 2\phi + \left(\frac{1}{3}\eta_{1,2}^\alpha \pm \eta_1^{\gamma 1} \pm \lambda^{\gamma 2} - \frac{1}{2}\eta_{2,2}^\alpha \right) \cos 2\phi \right. \\
&\quad \left. \pm \lambda^{\gamma 4} \cos 4\phi + \left(\frac{1}{3}\lambda_{1,66}^\alpha - \frac{1}{2}\lambda_{2,66}^\alpha \right) \cos 6\phi \right. \\
&\quad \left. \pm \eta_0^\gamma + \frac{1}{3}(\lambda_{1,2}^\alpha + \lambda_{1,4}^\alpha + \lambda_{1,6}^\alpha + \eta_{1,0}^\alpha) - \frac{1}{2}(\lambda_{2,2}^\alpha + \lambda_{2,4}^\alpha + \lambda_{2,6}^\alpha + \eta_{2,0}^\alpha) \right\}, \\
\bar{\varepsilon}_{\zeta\zeta} &= \left\{ \frac{1}{3}(\lambda_{1,2}^\alpha + \lambda_{1,4}^\alpha + \lambda_{1,6}^\alpha + \eta_{1,0}^\alpha) + \lambda_{2,2}^\alpha + \lambda_{2,4}^\alpha + \lambda_{2,6}^\alpha + \eta_{2,0}^\alpha \right. \\
&\quad \left. + (\eta_{2,1}^\alpha + \frac{1}{3}\eta_{1,1}^\alpha) \sin 2\phi + (\eta_{2,2}^\alpha + \frac{1}{3}\eta_{1,2}^\alpha) \cos 2\phi \right. \\
&\quad \left. + (\lambda_{2,66}^\alpha + \frac{1}{3}\lambda_{1,66}^\alpha) \cos 6\phi \right\} \\
\bar{\varepsilon}_{\xi\eta} &= \frac{1}{3} \{ (\eta_1^{\gamma 2} + \lambda^{\gamma 2}) \sin(2\phi) + \eta_2^\gamma \cos(2\phi) - \lambda^{\gamma 4} \sin(4\phi) + \eta_2^\gamma \}.
\end{aligned} \tag{6}$$

Note that, although they can be similarly obtained, we have not displayed the formulae giving the c -axis shear strains (the ε -strains related to the Cartesian strains $\bar{\varepsilon}_{\xi\zeta}$ and $\bar{\varepsilon}_{\eta\zeta}$), since we will not need them to analyse the magnetostriction measurements within the basal plane of the hcp structure. The latter also means that equations (6) should be particularized to $\theta = \pi/2$ when used to explain magnetostriction experiments where saturation magnetization lies on the basal plane, which is the case of the measurements on Tb, Dy and Ho that we will analyse next.

2. Analyses of the experimental results

The magnetostriction coefficients given in (5) are expressed in terms of microscopic parameters, since we obtained them starting from ionic Hamiltonians. Now, to compare with experimental results, we should convert the elastic and magnetoelastic constants from values per ion to GPa. Also, it is necessary to evaluate the thermal averages of the different spin operators appearing in (5).

At saturation, with the magnetization parallel to the z -axis, the thermal averages of the Stevens operators $\langle O_l^0 \rangle_T$ can be approximated as follows [4, 17]:

$$\langle O_l^0(\mathbf{J}) \rangle_T = c_l J^{(l)} \frac{I_{l+1/2} \{ \mathcal{L}^{-1}[m(T)] \}}{I_{1/2} \{ \mathcal{L}^{-1}[m(T)] \}} \equiv c_l J^{(l)} \hat{I}_{l+1/2} \{ \tilde{m} \}, \tag{7}$$

where $\hat{I}_{l+1/2} \{ \tilde{m} \}$ is the reduced hyperbolic Bessel function of $\mathcal{L}^{-1}[m(T)] \equiv \tilde{m}$, which is the inverse Langevin function of the reduced magnetization $m(T) = m(T)/m(0)$, c_l are numerical constants and $J^{(l)} \equiv J(J-1)(J-1/2) \dots [J-(l-1)/2]$. Furthermore, the unique non-null two-ion spin operators depend on temperature as the square of the reduced magnetization does [9], i.e. $\langle J_{zi} J_{zj} \rangle_T \simeq [m(T)]^2$.

Therefore, the explicit thermal dependence of the basal-plane strain obtained from (6) reads

$$\begin{aligned}
\bar{\varepsilon}_{\xi\xi} - \bar{\varepsilon}_{\eta\eta} &= \frac{2}{c_\gamma} \left\{ B_{\gamma 2}^2 P_2^2(\cos \theta) \hat{I}_{5/2} \{ \tilde{m} \} + B_{\gamma 2}^4 P_4^2(\cos \theta) \hat{I}_{9/2} \{ \tilde{m} \} \right. \\
&\quad \left. + B_{\gamma 2}^6 P_6^2(\cos \theta) \hat{I}_{13/2} \{ \tilde{m} \} + \left(\frac{D_{\gamma 1}}{6} \right) m^2 P_2^2(\cos \theta) \right\} \cos 2\phi \\
&\quad + \frac{2}{c_\gamma} \{ B_{\gamma 4}^4 P_4^4(\cos \theta) \hat{I}_{9/2} \{ \tilde{m} \} + B_{\gamma 4}^6 P_6^4(\cos \theta) \hat{I}_{13/2} \{ \tilde{m} \} \} \cos 4\phi, \tag{8}
\end{aligned}$$

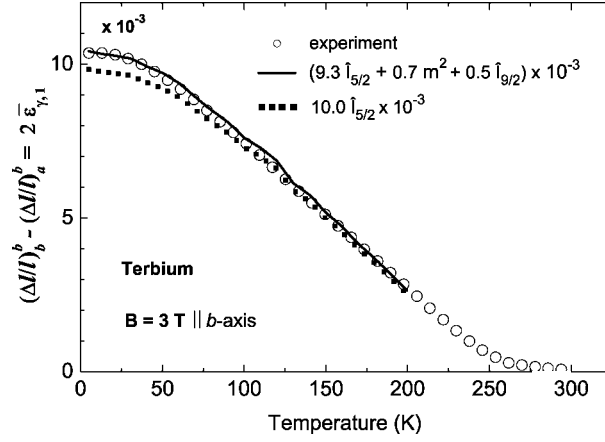


Figure 1. Two times the basal-plane symmetry-breaking irreducible strain $\bar{\epsilon}_{\gamma 1}$ for Tb (experimental data interpolated from [1]). The lines are fittings by using only a second-order single-ion CEF term (\cdots) and second- and fourth-order single-ion CEF and exchange terms in the magnetoelastic energy (—).

where macroscopic magnetoelastic constants B_{Γ}^l and D_{Γ} are related to the corresponding microscopic ones.

2.1. Basal plane magnetostriction of terbium

The measurements performed at 3 T by Rhyne and Legvold [1] within the basal plane of a single crystal of Tb allowed them to obtain the different magnetostriction constants expressed in Mason's notation. To make a re-analysis of these experiments in terms of our previous considerations, emphasizing the thermal dependence of the different magnetoelastic constants, we have taken Rhyne's experimental data obtained at temperatures between 350 and 4 K for the strains measured along the b and a hcp axes, when the sample was under a 3 T magnetic field applied along the easy b -axis. Since the experimental data were not obtained at exactly the same temperatures along both measuring directions, we used an interpolation procedure to get the deformation values along b and a axes at equally spaced temperatures. We plot in figure 1 the difference between the strains so obtained along both directions, as a function of temperature. Notice that the thermal expansion contribution to the strains is eliminated by this subtraction; therefore, we can equate its result to the difference of magnetostrictive strains $\bar{\epsilon}_{\xi\xi} - \bar{\epsilon}_{\eta\eta}$, obtained from (8), taking $\theta = \pi/2$ and $\phi = 0$. Thus,

$$\begin{aligned} \left[\frac{\Delta l}{l} \right]_{\text{gauge} \parallel b\text{-axis}}^{H \parallel b\text{-axis}} - \left[\frac{\Delta l}{l} \right]_{\text{gauge} \parallel a\text{-axis}}^{H \parallel b\text{-axis}} &= \bar{\epsilon}_{bb} - \bar{\epsilon}_{aa} = 2(\eta_1^{\gamma 1} + \lambda^{\gamma 2} + \lambda^{\gamma 4}) \\ &= \frac{2}{c_{\gamma}} \left[\left(\frac{D_{\gamma 1}}{4} \right) m^2 + B_{\gamma 2}^2 \hat{I}_{5/2}\{\tilde{m}\} + (B_{\gamma 2}^4 + B_{\gamma 4}^4) \hat{I}_{9/2}\{\tilde{m}\} \right. \\ &\quad \left. + (B_{\gamma 2}^6 + B_{\gamma 4}^6) \hat{I}_{13/2}\{\tilde{m}\} \right] \end{aligned} \quad (9)$$

(note that the above difference of relative deformations is two times the basal-plane symmetry-breaking irreducible strain $\bar{\epsilon}_{\gamma 1}$).

Table 1. Basal-plane magnetoelastic parameters (in MPa) for Tb, Dy and Ho deduced from the temperature dependence of the corresponding orthorhombic distortions of the basal plane under an applied magnetic field of 3 T.

	$B_{\gamma 2}^2$	$B_{\gamma 2}^4$	$B_{\gamma 4}^4$	$D_{\gamma 1/4}$
Tb	471	70	-45	36
Dy	375	96	0	22
Ho	119	802	-842	64

We have tried to fit the experimental data shown in figure 1 considering that only the terms of (9) depending on temperature as m^2 , $\hat{I}_{5/2}\{\tilde{m}\}$ and $\hat{I}_{9/2}\{\tilde{m}\}$ contribute in a wide enough range of temperatures; the sixth-order terms, which depend on temperature via a $\hat{I}_{13/2}\{\tilde{m}\}$ function, decrease as strongly as $[m(T)]^{21}$, and can have an appreciable contribution only at very low temperatures. The fit, which is also shown in figure 1, was done by using the magnetization values given in [18]; from it we get the values of the coefficients of the reduced Bessel functions $2B_{\gamma 2}^2/c_\gamma$ and $2(B_{\gamma 2}^4 + B_{\gamma 4}^4)/c_\gamma$, as well as the magnetoelastic exchange coefficient by multiplying with m^2 (see figure 1). By using the value of the elastic constant $c_\gamma = 101.2$ GPa at 0 K [19], we can directly obtain the values of $B_{\gamma 2}^2$ and $D_{\gamma 1/4}$, which are shown in table 1. However, from the magnetostriction measurements alone, we cannot separate the values of the two fourth-order macroscopic magnetoelastic parameters $B_{\gamma 2}^4$ and $B_{\gamma 4}^4$, which appear in different magnetostriction constants, according to the symmetry, but share the same temperature dependence. We need another type of experimental results where the magnetoelastic coupling will be revealed, as in the case of magnetic anisotropy measurements. As it can be shown [4], the sixfold magnetic anisotropy in the basal plane has magnetocrystalline and magnetoelastic contributions:

$$K_6^6(T) = [K_{6,MCME}^6 \hat{I}_{13/2}\{\tilde{m}(T)\} + K_{6,ME}^6 \hat{I}_{5/2}\{\tilde{m}(T)\} \hat{I}_{9/2}\{\tilde{m}(T)\}], \quad (10)$$

where $K_{6,MCME}^6$ is a magnetic anisotropy constant that is the sum of the pure magnetocrystalline anisotropy constant $K_{6,MC}^6$ plus a magnetoelastic anisotropy one, $-B_{\gamma 2}^4 B_{\gamma 4}^4/c_\gamma$, both having essentially a $\hat{I}_{13/2}\{\tilde{m}(T)\}$ temperature dependence [20]. The other magnetoelastic contribution $K_{6,ME}^6$ is related to the magnetoelastic parameters $B_{\gamma 2}^2$ and $B_{\gamma 4}^4$ as

$$K_{6,ME}^6 = -\frac{B_{\gamma 2}^2 B_{\gamma 4}^4}{c_\gamma}. \quad (11)$$

From magnetization measurements performed in a Tb single crystal [10, 18], by fitting to the law given by (10) the temperature dependence of the experimentally determined K_6^6 values (see figure 2), we have deduced magnetoelastic anisotropy constants $K_{6,ME}^6 = 0.21$ MPa and $K_{6,MCME}^6 = -0.02$ MPa. Once known in (11) the values of $K_{6,ME}^6$ and $B_{\gamma 2}^2$, the latter previously determined, we can obtain the value of $B_{\gamma 4}^4$, which is shown in table 1. This allows us to deduce the remaining fourth-order magnetoelastic parameter $B_{\gamma 2}^4$, which we tabulate, together with the others, in table 1. Now, it is also possible to obtain the value of $K_{6,MC}^6 = K_{6,MCME}^6 + B_{\gamma 2}^4 B_{\gamma 4}^4/c_\gamma$, which is -0.04 MPa.

Regarding the exchange magnetoelastic coupling parameter $D_{\gamma 1/4}$, it is less than 10% of the lowest order single-ion magnetoelastic parameter $B_{\gamma 2}^2$, which clearly indicates that the basal-plane magnetostriction of Tb has, mainly, a single-ion CEF origin.

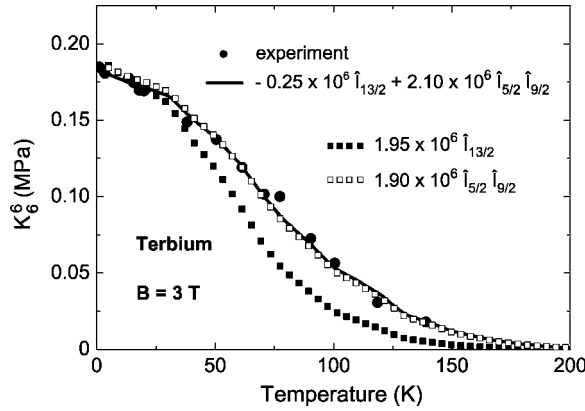


Figure 2. Basal-plane magnetic anisotropy constant for Tb (experimental data from [18]). The lines are fittings by using different temperature dependences as derived from the different magnetocrystalline and magnetoelastic contributions to the magnetic anisotropy (see text for details).

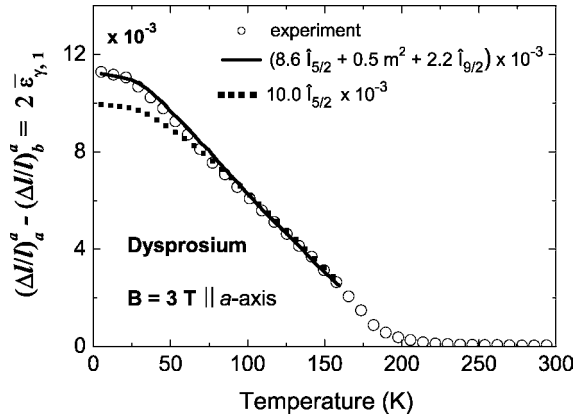


Figure 3. Two times the basal-plane symmetry-breaking irreducible strain $\bar{\epsilon}_{\gamma_1}$ for Dy (experimental data interpolated from [2, 10]). The lines are fittings by using only a second-order single-ion CEF term (\cdots) and second- and fourth-order single-ion CEF and exchange terms in the magnetoelastic energy (—).

2.2. Basal-plane magnetostriction of dysprosium

In figure 3 we display the difference between the strains measured along the easy \mathbf{a} -axis and the \mathbf{b} -axis of a Dy single crystal, under a magnetic field of 3 T applied along the easy axis, between RT and 4 K [2, 10]. These measurements, performed by Rhyne, were subsequently re-analysed by Martin and Rhyne [21], who determined the magnetostriction coefficients $\lambda^{\gamma,2}$ and $\lambda^{\gamma,4}$, concluding that the latter was practically negligible for the whole range of temperatures. They also obtained a relatively good agreement between the temperature dependence of $\lambda^{\gamma,2}$ obtained from the experimental data and the temperature variation given by $\hat{I}_{5/2}[\mathcal{L}^{-1}(m)]$, which is the dependence predicted by the second term of (9) (note that, for Dy, $2\bar{\epsilon}_{\gamma_1} = \bar{\epsilon}_{aa} - \bar{\epsilon}_{bb}$). However, the disagreement was considerable at low temperatures, where the high-order terms, not taken into account in that analysis, could be more relevant.

In our analysis of the above-mentioned magnetostriction experiments in Dy, we only neglected the sixth-order terms in (9), as we did for Tb, and considered the thermal variations associated with the second- and fourth-order magnetoelastic parameters to try to fit the temperature dependence of the basal-plane strain shown in figure 3. We used existent magnetization measurements [18] to calculate the values of the reduced Bessel functions at the different temperatures. The best fit obtained is shown in figure 3 where the values of $2B_{\gamma 2}^2/c_\gamma$ and $2(B_{\gamma 2}^4 + B_{\gamma 4}^4)/c_\gamma$, the reduced Bessel functions coefficients, are also displayed. The agreement is good in the whole range of temperatures, from 4 to 160 K, where magnetization data were available. The fact that the fourth-order magnetoelastic parameter $B_{\gamma 4}^4$ is negligible, according to Martin and Rhyne [21], allows us to directly obtain the other fourth-order parameter $B_{\gamma 2}^4$, which we tabulate, jointly with the $B_{\gamma 2}^2$ value obtained from the fit, in table 1 (we used the elastic constant $c_\gamma = 87.3$ GPa at 0 K [22]). Note that $B_{\gamma 4}^4$ is directly related to the magnetoelastic anisotropy (see (11)). This is corroborated when we are able to fit the experimental values of $K_6^6(T)$ for Dy [10, 18, 23] by using only the first term of equation (10) (which results to be the pure magnetocrystalline anisotropy if $B_{\gamma 4}^4 = 0$). The value that we obtain from this fit for the magnetocrystalline anisotropy constant is $K_{6,MC}^6 = -1.17$ MPa.

The exchange contribution to the magnetoelastic energy is of the same order as for Tb (see the value of $D_{\gamma 1}/4$ in table 1).

2.3. Basal plane magnetostriction of holmium

Concerning the magnetization easy direction within the basal plane, holmium has the same as terbium, the \mathbf{b} -axis, but the former possesses a very much complex magnetic structure [4, 10]. The magnetostriction of single-crystal Ho, measured in fields up to 3 T and between RT and 4 K by Rhyne *et al* [3] reflects such a complexity; in the temperature dependences of the different strains measured, clear anomalies are observed not only at the Néel and ferro-cone transition temperatures (132 and about 20 K, respectively), but also at around 70 K, where no magnetic phase changes have been reported. In a previous work [24], we measured the basal-plane magnetoelastic stresses in epitaxial (0001) Ho films (5000 and 10000 Å thick), which showed the paramagnetic-helix transition, but not the transition to the ferro-cone phase. We also measured the magnetic anisotropy within the basal plane in the 5000 Å Ho film, from 10 K up to above the Néel temperature, in fields up to 2 T and deduced the values of the magnetocrystalline and the magnetoelastic contributions [20] from the thermal variation of this anisotropy. We will make use of this and comment on the above magnetoelastic stress results later, in relation to the following analysis of the basal-plane magnetostriction in bulk Ho.

In figure 4, we display the difference between the strains measured along the easy \mathbf{b} -axis and the \mathbf{a} -axis, i.e. $2\bar{\varepsilon}_{\gamma 1} = \bar{\varepsilon}_{bb} - \bar{\varepsilon}_{aa}$, of Ho single crystal under a magnetic field of 3 T applied along the easy axis, and between RT and 4 K [3]. The thermal variation of $\bar{\varepsilon}_{\gamma 1}$ displays a much less regular behaviour than that observed for Tb and Dy, exhibiting a small anomaly at around 25 K and a drastic change from the previous trend between 70 and 100 K. In this case, we have performed the same analysis as before, but trying to fit the experimental results only for temperatures below 70 K. Again, we considered exchange and second- and fourth-order single-ion magnetoelastic contributions in (9) and obtained the fit shown in figure 4. Its quality is reasonable within that low-temperature range. The values of $B_{\gamma 2}^2$ and $D_{\gamma 1}/4$ are directly obtained from the fitting by using the value of $c_\gamma = 106.6$ GPa at 0 K [22]. Now, from the above-mentioned magnetic anisotropy measurements performed within the basal plane of a 5000 Å Ho film, we have obtained that $K_{6,ME}^6 = 0.94$ MPa (note that the 5000 Å film behaves practically as the bulk material [24] and magnetic anisotropy measurements performed in that film allow us to obtain $K_{6,ME}^6$ more accurately than using magnetization measurements made

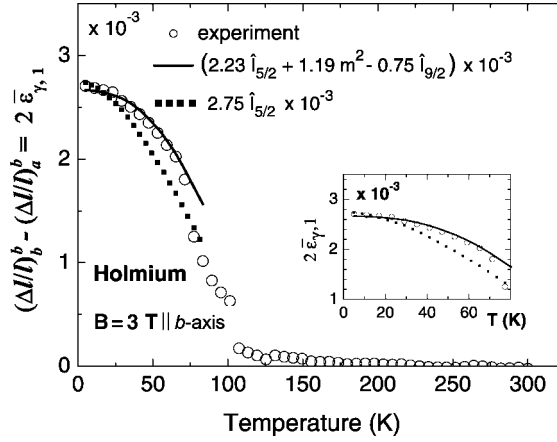


Figure 4. Two times the basal-plane symmetry-breaking irreducible strain $\bar{\epsilon}_{\gamma,1}$ for Ho (experimental data interpolated from [3]). The lines are fittings by using only a second-order single-ion CEF term (\cdots) and second- and fourth-order single-ion CEF and exchange terms in the magnetoelastic energy (—). The inset is a zoom of the low-temperature region.

in bulk Ho). By using this value, and that previously deduced for $B_{\gamma,2}^2$, we calculate $B_{\gamma,4}^4$ for Ho and, having it, we can separate the value of $B_{\gamma,2}^4$ from the remaining fitting parameter of $2\bar{\epsilon}_{\gamma,1}(T)$. The calculated value for $K_{6,MC}^6$ is -1.84 MPa. All the magnetoelastic parameters deduced for Ho are given in table 1. The sum of the different magnetoelastic stresses at 0 K, $(D_{\gamma,1}/4) + B_{\gamma,2}^2 + B_{\gamma,2}^4 + B_{\gamma,4}^4$, is 142 MPa, which is very close to the value of 137.5 MPa obtained from our magnetoelastic stress measurements performed in the 5000 Å thick Ho film ([24]; in this reference, cylindrical symmetry was assumed within the basal plane and, unlike in the present paper, a factor 1/2 in the definition of the magnetoelastic energy was used). Note that, in this case, the exchange contribution to the magnetoelastic energy, $D_{\gamma,1}/4$, is about 50% of the single-ion term $B_{\gamma,2}^2$. Moreover, if we consider all of the single-ion contributions, the exchange term represents almost half of the total magnetoelastic energy.

3. Discussion and conclusions

From the re-analysis of existent magnetostriction experiments within the basal plane of terbium, dysprosium and holmium, we have been able to obtain satisfactory agreements between the experimental results and the predictions of the standard theory of magnetostriction, particularized in our analyses to the regime of magnetization saturated along the field direction. Moreover, we have determined high-order single-ion magnetoelastic parameters which, in some cases, are by no means negligible as compared with the lowest order one, $B_{\gamma,2}^2$, associated with the magnetostriction coefficient $\lambda^{\gamma,2}$. We have seen that, in the thermal variation of the basal-plane orthorhombic strain $\bar{\epsilon}_{\gamma,1}$, related to the second- and fourth-order magnetostriction coefficients $\lambda^{\gamma,2}$ and $\lambda^{\gamma,4}$, different thermal dependencies related to the order of the Stevens angular momentum operator to which they are connected are involved. This represents a clear distinction between these magnetostriction coefficients, associated with the γ strains, and those linked with the α -strains (note that the exchange magnetostriction contributions have, at saturation, the same temperature dependence for both kinds of strains). The origin of such a difference is due to the fact that the α -strains do not break the hexagonal symmetry within the basal plane of the hcp structure, whereas the γ -strains do it, giving rise to lower symmetries, of

second and fourth order. Since a second-order symmetry, from a quantum-mechanical point of view, can arise from Stevens operators of order $l = 2, 4$ and 6 , and a fourth-order one, from $l = 4$ and 6 operators, it is clear why the appearance of symmetries lower than the hexagonal one can produce a mixture of temperature dependences in the γ -strains. We have seen that it is necessary to include such high-order terms to account for the basal-plane magnetostriction of Tb and Dy in a wide range of temperatures, from low temperature up to near T_N and, to explain the case of Ho from low temperature up to about half of T_N .

The comparison of the different magnetoelastic parameters shown in table 1 indicates, first of all, that for Tb and Dy the exchange magnetoelastic energy is less than one order of magnitude smaller than the single-ion contribution to the total magnetoelastic energy, whereas in Ho the exchange contribution represents a significant part of it. This indicates that the modulation by the strain of the spin-interaction exchange energy plays an important role in the magnetostriction of holmium, as it was previously deduced from x-ray diffraction experiments [12], but for Tb and Dy it is the dependence on the strain of the single-ion CEF interaction which dominates the magnetoelastic behaviour, although some exchange contribution is observed, in agreement with former evidence deduced from magnetostriction measurements at the paramagnetic regime [11].

We also see, in table 1, a regular tendency for the second-order parameter $B_{\gamma 2}^2$, which decreases from Tb to Ho, opposite to the behaviour of the fourth-order parameter $B_{\gamma 2}^4$, which increases with the atomic number, being the largest one for the Ho. Interestingly, the $B_{\gamma 4}^4$ fourth-order magnetoelastic stress parameter is also very large for Ho, which is the cause of the very large magnetoelastic contributions to the magnetic anisotropy within the basal plane of Ho; recall that the magnetoelastic anisotropy constants are $-B_{\gamma 2}^4 B_{\gamma 4}^4 / c_\gamma = 2.50$ MPa and $K_{6,ME}^6 = 0.94$ MPa, the sum of both being comparable with the pure magnetocrystalline constant $K_{6,MC}^6 = -1.84$ MPa. For Tb, the dominant magnetic anisotropy is the magnetoelastic one (recall that $K_{6,MC}^6 = -0.04$ MPa and the magnetoelastic contributions to the anisotropy energy amount to 0.21 MPa, $K_{6,ME}^6$, plus 0.019 MPa, $-B_{\gamma 2}^4 B_{\gamma 4}^4 / c_\gamma$). The opposite is observed for Dy, in which the anisotropy has a pure CEF origin ($K_{6,MC}^6 = -1.17$ MPa, the magnetoelastic anisotropy contributions being negligible). This special circumstance occurring in Ho, in which both contributions have similar weights, is, in our opinion, the main reason for the much more complex magnetic behaviour shown by holmium as compared with terbium or dysprosium. It should be taken into account that the magnetoelastic anisotropy energy is a field-dependent contribution to the free energy of the system, unlike the case of the magnetocrystalline anisotropy contribution and, therefore, the sum of both terms can be different at different applied magnetic fields in Ho in a much greater extent than in Tb or Dy. On the other hand, the large magnetoelastic contribution to K_6^6 in Ho can help in understanding why the basal-plane anisotropy in this element is 10% of the axial term K_2 , the largest percentage in the series Tb, Dy and Ho [10].

Acknowledgments

We acknowledge the financial support of Spanish MCyT under grants MAT2000-1290-C03-01 and MAT2003-00893. LB thanks Fundación Ramón Areces for a predoctoral grant.

References

- [1] Rhyne J J and Legvold S 1965 *Phys. Rev. A* **138** 507–14
- [2] Rhyne J J 1965 *PhD Thesis* Iowa State University
- [3] Rhyne J J, Legvold S and Rodine E T 1967 *Phys. Rev.* **154** 266–9

- [4] Jensen J and Mackintosh A R 1991 *Rare Earth Magnetism: Structure and Excitations* (Oxford: Clarendon Press)
- [5] Flynn C P and Salomon M B 1996 *Handbook of the Physics and Chemistry of Rare Earths* vol 22, ed K A Gschneidner and L R Eyring (Amsterdam: North-Holland)
- [6] Ciria M, Arnaudas J I, del Moral A, Tomka G J, de la Fuente C, de Groot P A J, Wells M R and Ward R C C 1995 *Phys. Rev. Lett.* **75** 1634
- [7] Arnaudas J I, del Moral A, Ciria M, de la Fuente C, Ward R C C and Wells M R 1998 *Frontiers in Magnetism of Reduced Dimension Systems* ed V G Baryakhtar, P E Wigen and N A Lesnik (Dordrecht: Kluwer) pp 525–52
- [8] Callen E R and Callen H B 1963 *Phys. Rev.* **129** 578
- [9] Callen E and Callen H B 1965 *Phys. Rev. A* **139** 455
- [10] Rhyne J J 1972 *Magnetic Properties of Rare Earth Metals* ed R J Elliot (New York: Plenum Press) pp 129–85
- [11] Boutron P 1971 *J. Phys. Chem. Solids* **33** 1005–15
- [12] Ohsumi H 2002 *J. Phys. Soc. Japan* **71** 1732–9
- [13] Rotter M, Doerr M, Loewenhaupt M and Svoboda P 2002 *J. Appl. Phys.* **91** 8885–7
- [14] Divis M, Lukac P and Svoboda P 1990 *J. Phys.: Condens. Matter* **37** 7569–73
- [15] Buck S and Fähnle M 1998 *Phys. Rev. B* **57** 044–7
- [16] Hutchings M T 1964 *Solid State Phys.* **6** 227–73
- [17] Callen E R and Callen H B 1960 *J. Phys. Chem. Solids* **16** 310
Callen H B and Callen E R 1966 *J. Phys. Chem. Solids* **27** 1271–85
- [18] Féron J L 1969 *PhD Thesis* Université de Grenoble
- [19] Palmer S B, Lee E W and Islam M N 1974 *Proc. R. Soc. A* **338** 341
- [20] Benito L 2004 *PhD Thesis* Universidad de Zaragoza
- [21] Martin D J and Rhyne J J 1977 *J. Phys.: Condens. Matter* **10** 4123–26
- [22] Palmer S B 1970 *J. Phys. Chem. Solids* **31** 143
- [23] Liu S H, Behrendt D R, Legvold S and Good R H Jr 1959 *Phys. Rev.* **116** 1464–68
- [24] Ciria M, Arnaudas J I, del Moral A, Wells M R and Ward R C C 1998 *Appl. Phys. Lett.* **72** 2044–46